Dynamic-light-scattering study of glasses of hard colloidal spheres

W. van Megen and S. M. Underwood*

Department of Applied Physics, Royal Melbourne Institute of Technology, Melbourne, Victoria 3000, Australia
(Received 3 June 1992)

Dynamic light scattering is applied to the glass phase of nonaqueous suspensions of sterically stabilized colloidal spheres. The short-ranged steric repulsion ensures that the particle interactions are close to hard sphere. This is supported by the observation that the equilibrium phase behavior of these suspensions agrees with that predicted for the hard-sphere atomic system. We verify a model for a nonergodic medium, which assumes that the particles are localized during an experiment and which allows the intermediate scattering function to be calculated from a single measurement of the time-averaged intensity autocorrelation function. Intermediate scattering functions are obtained for several concentrations over a range of wave vectors around the main diffraction peak. The measured nonergodicity parameters are in good agreement with the predictions of mode-coupling theory for the hard-sphere glass. The comparison involves no adjustable parameters. At long times the intermediate scattering functions can be scaled to a single curve for over 2.5 decades in time. This, combined with the results that the nonergodicity parameters and critical amplitudes required for the scaling are in quantitative agreement with mode-coupling theory, provides a convincing verification of the predicted factorization property of the β process in the glass phase.

PACS number(s): 64.70.Pf, 61.20.Ne, 82.70.Dd

I. INTRODUCTION

Suspensions of near-micrometer-sized spheres are interesting and extremely useful replicas of atomic fluids and solids. They exhibit a transition from a fluidlike phase to a crystalline phase evident by the iridescence caused by the Bragg reflections from lattice planes with spacing comparable to the wavelength of visible light [1]. Importantly, due to their slow structural relaxation times, colloidal suspensions are also easily concentrated to dense metastable states without crystallization occurring [1–3]. Suspensions of identical spherical particles are therefore valuable materials for studying fundamental aspects of the glass transition.

The significant upsurge of interest in the glass transition, witnessed in the past few years [4], has been catalyzed by the predictions of mode-coupling theory. This theory provides a detailed description of the microscopic dynamics of supercooled liquids around the glass transition [5–8]. Its key feature is the inclusion, in the equations of motion, of a delayed nonlinear coupling between density fluctuations. Increase of this coupling by *continuously* varying the parameters that control the static properties produces a sharp crossover of the dynamics from fluidlike to solidlike, i.e., an ergodic to nonergodic transition at which a fraction of the fluid structure is arrested. On approaching the transition two slow structural relaxation processes are predicted with critically diverging time scales. The slower α process arrests at the transition while the faster decay, the β process, describes a localized motion that persists into the nonergodic glass phase. Mode-coupling theory applies to the so-called "fragile" glass formers [9] where the slowing of structural relaxation and ultimate structural arrest on supercooling are purported to be the mechanism for the strong non-

Arrhenius temperature or density dependence of the viscosity. However, the sharp transition is only predicted when phonon-activated hopping motions, the usual mechanism for the restoration of ergodicity in molecular glasses, are excluded. Their inclusion will round and perhaps obscure the sharp transition predicted by the basic version of the theory.

The picture that has emerged of the particle motion in a dense fluid is one of a sequence of temporary entrapments in ephemeral neighbor cages. Small-scale motion within the cage may be relatively easy but a larger-scale excursion requires the cooperative motion of a larger number of particles. Since a caged particle is itself a constituent of another cage, small- and large-scale concentration fluctuations are inextricably coupled. With increasing concentration, increasingly large structural adjustments are required for a given particle to escape from its cage. The coupling leads to an increase and ultimate divergence of the structural relaxation time, the permanent trapping of particles, and the arrest of concentration fluctuations of all spatial scales.

The predictions of mode-coupling theory have led to a reappraisal of experimental data on supercooled fluids [8] and have provoked a spate of light scattering and neutron scattering experiments in systems of mixed ions [10], polymers [11], and van der Waals molecules [12] around the glass transition. The results are generally consistent with the theory; experimental evidence for a two-step decay of the density fluctuations at long times, beyond those corresponding to microscopic or vibrational motions, provides strong support for the theory. However, as possible consequences of hopping motions [4,13] or the complex nature of the materials, necessarily chosen to prevent crystallization on supercooling, the comparisons between experiment and mode-coupling theory are not without am-

biguity. Difficulties also arise in unambiguously discriminating the two predicted relaxation processes [13]. Computer simulation, the standard recourse for testing theories of condensed matter, has the added problem of limited accuracy due to the restricted sampling of phase space associated with the very slow structural rearrangements in fluids near the glass transition [14]: It is effectively impossible to obtain proper canonical averages in the nonergodic glass phase.

Nonaqueous suspensions of spherical particles, with narrow size distributions, stabilized by thin steric barriers can be prepared so that the particle interaction is close to that of hard spheres. Their phase behavior [1,15,16] is in accord with computer simulation and theory for the hypothetical hard-sphere atomic system. The size disparity (about 10^3) between near-micrometer-sized colloidal particles and atoms has two significant consequences: First, the shear moduli of crystals of colloidal particles are about 10 orders of magnitude smaller than those of atomic crystals. Thus the shear stresses imposed by simply tumbling a sample are sufficient to destroy or "melt" a crytallized suspension to a metastable phase. Second, the motions of colloidal particles are slower than those of atoms by a similar margin so that, with the possible exception of those states very close to the (equilibrium) melting concentration, structural recovery (of the metastable fluid to crystal) takes long enough to allow the study of the structure and dynamics of the metastable phases. Importantly, a fluidlike suspension can easily be concentrated to a dense long-lived amorphous phase without the intervention of crystallization [2,3]. By contrast simple atomic systems cannot be cooled or compressed rapidly enough to by-pass crystallization and still attain controllable glass phases. These characteristics suggest that suspensions, comprising identical spherically interacting units, constitute the simplest systems to show a glass transition. Moreover, since the diffusive motions of suspended particles are strongly overdamped, phonon-induced hopping motions are suppressed and could possibly be absent. Thus these suspensions may well exhibit the best experimental illustration of the sharp transition from an ergodic fluid to an ideal glass predicted by the basic version of mode-coupling theory [7].

The particle dynamics of colloidal suspensions, as expressed by the intermediate scattering function (the autocorrelation function of the particle number density fluctuations), can be measured by dynamic light scattering (DLS). This technique is ideally suited to probe the structure and dynamics on the spatial $[O(10^{-7} \text{ m})]$ and temporal $[O(10^{-4} \text{ s})]$ scales of the microscopic diffusive motions of suspended particles [17]. The longest delay time (exceeding 1000 s) attainable with modern purpose-built correlators, is limited only by the long-term stability of the samples, optical equipment, and, of course, the patience of the experimentalist; a dynamic range of over eight decades is readily obtained in a single experiment. In this sense DLS applied to colloidal suspensions is more straightforward than, although analogous to, neutron scattering applied to molecular fluids. In the latter the results of two different spectrometers must be combined in order to obtain a dynamic range of more than four de-

cades [18]. We mention in passing that, like dynamic neutron scattering [19], DLS allows measurement of the coherent intermediate scattering function (collective particle concentration fluctuations) and also, by using suspensions of dynamically identical but optically contrasting particles, the incoherent intermediate scattering function (single-particle motion) [20].

The feature that distinguishes DLS from other spectroscopic techniques is that it follows, through the measurement of the time-averaged time autocorrelation function $\langle I(q,0)I(q,t)\rangle_T$ of the scattered intensity, the temporal evolution of the squared amplitude of a *single* spatial Fourier component of the particle number density fluctuations [21,22]. Special procedures must therefore be adopted when the dynamic properties of a nonergodic sample, such as a colloidal glass, are measured by DLS. One approach is to construct the ensemble average by a "brute force" procedure that entails accumulating data for a large number of independent scattering volumes in the sample. This procedure was used in the first DLS measurements on glasses of hard-sphere suspensions [2,3]. It is, however, extremely tedious and prone to significant systematic statistical uncertainties. Since then Pusey and van Megen [21] have proposed a model for a nonergodic medium in which the particles are constrained to move about an amorphous distribution of fixed average positions. This model effectively allows the calculation of the (ensemble-averaged) intermediate scattering function from a single measurement of the time-averaged intensity autocorrelation function.

Previous work [2,3] on colloidal suspensions of hard spherical particles has established a close connection between the concentration at which homogeneously nucleated crystallization is first suppressed and that at which the intermediate scattering function, measured by DLS in the amorphous phase, no longer decays fully. Moreover, the arrest of concentration fluctuations, indicated by DLS, occurs over a very narrow range of concentration. Significantly, there is no qualitative change in the static structure factor of the metastable fluids over this concentration range. The intermediate scattering functions obtained in these experiments, particularly on the fluid side of the glass transition, could be scaled to the master functions of the α and β processes calculated by mode-coupling theory for the hard-sphere system [23,24]. In addition, the scaling times and amplitudes of these processes satisfied the predicted scaling laws.

In this paper we present a detailed account of DLS measurements on colloidal glasses, concentrating particularly on the wave-vector dependence of the intermediate scattering functions. A preliminary account of aspects of this work has already been published [25]. The objectives here are (i) to verify the model and DLS theory for nonergodic media, thereby demonstrating that the particles in a colloidal glass are effectively localized over the duration of an experiment, and (ii) to use the model to determine the intermediate scattering functions of colloidal glasses over a range of scattering vectors and particle concentrations and compare the results with the predictions of mode-coupling theory.

In the following section of this paper we outline the

theory of DLS by nonergodic media and give a brief account of the relevant aspects of mode-coupling theory. In Sec. III the experimental procedures are summarized. Experimental results are presented and discussed in Sec. IV which includes a description of the visual behavior of the suspensions, verification of the model for a nonergodic medium, and comparison of DLS results on colloidal glasses with mode-coupling theory. Concluding remarks are presented in Sec. V.

II. THEORY

A. Dynamic light scattering

Dynamic light scattering [17,22] measures the normalized time-averaged time autocorrelation function of the scattered intensity

$$g_T^{(2)}(q,\tau) = \langle I(q,0)I(q,\tau) \rangle_T / \langle I(q) \rangle_T^2 \ . \tag{1}$$

The magnitude of the scattering vector, $\mathbf{q}$ is $q = (4\pi n / \lambda)\sin(\theta/2)$, where λ is the vacuum wavelength of the radiation, n the refractive index of the medium, and θ the scattering angle. For an ergodic medium the scattered intensity, $I(q,t)$, undergoes, in the course of an experiment of duration T, the full range of fluctuations consistent with the full ensemble of spatial configurations accessible to the N particles in the scattering volume V. In this case the measured time-averaged intensity autocorrelation function, denoted by the brackets $\langle \ \rangle_T$ in Eq. (1), is equivalent to its ensemble average $\langle \ \rangle_E$, i.e.,

$$g_T^{(2)}(q,\tau) = g_E^{(2)}(q,\tau) \ . \tag{2}$$

Since the scattered light field has Gaussian statistical properties, the measured intensity autocorrelation function is related to the normalized ensemble-averaged autocorrelation function of the scattered light field, $f(q,\tau)$, or intermediate scattering function (ISF), by the usual Siegert relationship [17,22],

$$g_E^{(2)}(q,\tau) = 1 + c[f(q,\tau)]^2 \ . \tag{3}$$

Here, c is an experimental constant proportional to the ratio of the coherence area, or speckle size, to the detector area. The ISF is given by

$$f(q,\tau) = F(q,\tau)/F(q,0) \ , \tag{4}$$

where

$$F(q,\tau) = \langle E(q,0)E^*(q,\tau) \rangle_E \ , \tag{5}$$

and $F(q,0) = S(q)$ is the static structure factor. For N identical spherical particles located at $\mathbf{r}_j(t)$ and suspended in an optically homogeneous background the instantaneous amplitude of the scattered light field is (in the far-field limit)

$$E(q,t) = \sum_{j=1}^{N} \exp[i\mathbf{q}\cdot\mathbf{r}_j(t)] \ . \tag{6}$$

This quantity represents the spatial Fourier component, of wave vector q, of particle concentration fluctuations $\delta\rho$, i.e., apart from constants which are canceled through normalization [as in Eq. (4)],

$$E(q,t) = \delta\rho(q,t)$$
$$= \int \delta\rho(\mathbf{r},t)\exp[i\mathbf{q}\cdot\mathbf{r}(t)]d^3r \ . \tag{7}$$

We reiterate that in the ergodic case the particles have sufficient freedom that in an experiment of "reasonable" duration all values, between 0 and 2π, of the phase factors, $\mathbf{q}\cdot\mathbf{r}_j(t)$, are effectively sampled. Then $E(q,t)$ constitutes a zero-mean complex random Gaussian variable.

In a nonergodic medium, such as the colloidal glass considered in this paper, the particles are partly constrained. Consequently, the scattered field is no longer a zero-mean random Gaussian variable and the ensemble-averaged intensity autocorrelation function is not realized in a single measurement (i.e., $\langle \ \rangle_T \neq \langle \ \rangle_E$). A corollary to this is that the (ensemble-averaged) ISF cannot be obtained from the measured time-averaged intensity autocorrelation function with the use of Eq. (3).

One approach to DLS by a nonergodic medium is to determine the ensemble average, $g_E^{(2)}(q,\tau)$, by accumulating data for a very large number of independent scattering volumes in the sample [2,3]. An alternative, proposed by Pusey and van Megen [21], to this tedious procedure is to model a nonergodic medium by writing

$$\mathbf{r}_j(t) = \mathbf{R}_j + \boldsymbol{\Delta}_j(t) \ , \tag{8}$$

where $\mathbf{R}_j$ is the fixed average position of particle j and $\boldsymbol{\Delta}_j(t)$ is its (time-dependent) displacement about this position. This assumption allows the scattered field to be expressed as the sum of fluctuating, E_F, and constant, E_C, components,

$$E(q,t) = E_F(q,t) + E_C(q,t) \ , \tag{9a}$$

$$E_F = \sum_{j=1}^{N} \exp(i\mathbf{q}\cdot\mathbf{R}_j)\{\exp[i\mathbf{q}\cdot\boldsymbol{\Delta}_j(t)]$$
$$- \langle \exp[i\mathbf{q}\cdot\boldsymbol{\Delta}_j(t)] \rangle_T\} \ , \tag{9b}$$

$$E_C = \sum_{j=1}^{N} \exp(i\mathbf{q}\cdot\mathbf{R}_j)\langle \exp[i\mathbf{q}\cdot\boldsymbol{\Delta}_j(t)] \rangle_T \ . \tag{9c}$$

In contrast to the ergodic case considered above, the time average $\langle \ \rangle_T$ here indicates an average over the subensemble of configurations accessible to the particles in a particular volume of the sample. Particles in different volumes in the sample have different fixed average configurations $\{\mathbf{R}_j\}$ and yield different constant components in the scattered field [Eq. (9c)]. However, the fluctuating component is a zero-mean complex random Gaussian variable whose average properties are the same for all scattering volumes.

As shown in Ref. [21], these considerations of a nonergodic medium lead to the following relationship between the measured time-averaged intensity autocorrelation function, $g_T^{(2)}(q,\tau)$, and the normalized (ensemble-averaged) ISF, $f(q,\tau)$ [defined by Eq. (4) to (6)];

$$g_T^{(2)}(q,\tau)=1+Y^2[f(q,\tau)-f(q,\infty)]^2+2Y\{1-Y[1-f(q,\infty)]\}[f(q,\tau)-f(q,\infty)] \,, \tag{10a}$$

$$Y=I_E/I_T \,, \tag{10b}$$

where $I_T=\langle I(q,t)\rangle_T$ is the time-averaged total scattered intensity for the particular scattering volume under study and $I_E=\langle I(q,t)\rangle_E$ is the total scattered intensity averaged over an ensemble of different scattering volumes. Equation (10) can be solved to give

$$f(q,\tau)=1+Y^{-1}\{[g_T^{(2)}(q,\tau)$$
$$-g_T^{(2)}(q,0)+1]^{1/2}-1\} \,. \tag{11}$$

Taking the limit $\tau\rightarrow\infty$ in Eq. (11), and using the fact that intensity fluctuations become totally decorrelated at long times [i.e., $g_T^{(2)}(q,\infty)=1$], gives

$$f(q,\infty)=1+Y^{-1}\{[2-g_T^{(2)}(q,0)]^{1/2}-1\} \,. \tag{12}$$

In addition to the usual experimental requirements in DLS [17,22] the derivation of Eq. (10) assumes a detector area much smaller than one coherence area or speckle.

Two limiting cases of the above results can be considered. The first is an ergodic medium where the particles are able to execute large excursions $\{\Delta_j(t)\}$ so that $\langle\exp[i q\cdot\Delta_j(t)]\rangle_T=0$ and the constant component in the scattered field vanishes. The net scattered field, $E(q,t)$, is now a zero-mean random Gaussian variable with the consequences that $I_T=I_E$, $g_T^{(2)}(q,0)=2$, and Eq. (10) reduces to the familiar result for an ergodic medium, Eq. (3) (with $c=1$ due to the assumed point detector). Further, as may be seen from Eq. (12), $f(q,\infty)=0$, i.e., concentration fluctuations ultimately decay completely. The second case is the nonergodic extreme, such as a fully compressed glass, in which the randomly positioned particles are completely immobilized so that $\Delta_j(t)=0$ for all j. Now the fluctuating component of the scattered field vanishes and the scattered intensity is independent of time. The result is that $g_T^{(2)}(q,\tau)=1$ for all τ and one sees, from Eqs. (11) and (12), that $f(q,\tau)=f(q,\infty)=1$, i.e., the ISF is constant in time indicating that particle concentration fluctuations are completely frozen.

Generally the light scattered by a glass, such as the glass phase of hard spheres at concentrations below random close packing, comprises both a constant component, associated with the arrested structure, and a fluctuating component, associated with the restricted particle excursions about their fixed average positions. The fraction of the frozen structure (or nonergodicity parameter), $f(q,\infty)$, can be obtained, by using Eq. (12), from the measured mean-squared value, σ^2 [$\sigma^2=g_T^{(2)}(q,0)-1$], of the intensity fluctuations.

We emphasize that I_E and $f(q,\tau)$ are ensemble-averaged properties of the system and, as such, are independent of the particular volume being studied. However, the time-averaged measured quantities, I_T and $g_T^{(2)}(q,\tau)$ will, in general, be different for different scattering volumes in the sample. In particular, a large value for I_T (or bright speckle) implies a large value for the constant component of the scattered intensity and hence

a small value for the mean-squared intensity fluctuation [see Eq. (12)].

Furthermore, for a nonergodic medium the apparent short-time diffusion coefficient,

$$D_{\text{app}}(q)=-q^{-2}\lim_{\tau\rightarrow 0}\frac{\partial}{\partial\tau}\ln[g_T^{(2)}(q,\tau)-1]^{1/2} \,, \tag{13}$$

calculated directly from a first cumulant analysis of the measured time-averaged intensity correlation function, depends on the particular scattering volume and is, therefore, incorrect. The correct short-time diffusion coefficient, $D(q)$, must be calculated from the ISF:

$$D(q)=-q^{-2}\lim_{\tau\rightarrow 0}\frac{\partial}{\partial\tau}\ln[f(q,\tau)] \,. \tag{14}$$

As shown in Ref. [21], $D(q)$ is related to $D_{\text{app}}(q)$ by

$$D(q)=D_{\text{app}}(q)\sigma^2/Y \,. \tag{15}$$

From Eq. (14) it follows that the short-time result for the ISF is

$$f(q,\tau\rightarrow 0)=\exp[-D(q)q^2\tau] \,, \tag{16}$$

where, in analogy to the generalized Einstein equation, the wave-vector-dependent short-time diffusion coefficient can be expressed as a ratio of hydrodynamic and thermodynamic terms as follows [26]:

$$D(q)=H(q)/S(q) \,. \tag{17}$$

The hydrodynamic term, $H(q)$, is essentially a configurational average over the mobility tensor [26,27]. The latter couples the particle velocities with the forces exerted on them. Without hydrodynamic interactions $H(q)=1$ and Eq. (17) expresses the analog, in colloidal suspensions [28], of the de Gennes narrowing [29], the slowing of concentration fluctuations in the region of the diffraction maximum. For concentrated hard-sphere suspensions $H(q)$ is strongly concentration dependent [for example, near the freezing concentration $H(q\rightarrow 0)\simeq 0.02$ and $H(q>q_m)\simeq 0.3$, q_m is the position of the main peak in $S(q)$] and it has a q dependence qualitatively similar to the static structure factor [27,30]. Hence the compressibility, $S(q)$, that drives the concentration fluctuations is partly offset by hydrodynamic effects. For a hypothetical hard-sphere suspension at freezing with no hydrodynamic interactions the ratio $D(q_m)/D(0)=S(0)/S(q_m)$ has a value of about 0.007, whereas with the inclusion of the hydrodynamic interactions the corresponding ratio $D(q_m)/D(0)=H(q_m)S(0)/H(0)S(q_m)$ is around 0.15. Thus the hydrodynamic interactions cause considerable smearing of the wave-vector dependence of the decay rates of concentration fluctuations at short times.

B. Mode-coupling theory

The central aspect of recent application of mode-coupling theory to very dense supercooled fluids is the ex-

pression of the memory kernel, or autocorrelation function of the random force, in terms of products of conserved variables [7,8]. This kernel, $M(q,\tau)$, is essentially defined by the generalized Langevin equation. The latter is derived from either the Liouville [31] or Smoluchowski [32] equations through the application of projection operator formalism. The basic version of the theory includes only density fluctuations, i.e.,

$$M(q,\tau)= \sum_{q',q''} V(q;q',q'')f(q',\tau)f(q'',\tau) . \qquad (18)$$

Thus a density or concentration fluctuation of wave vector q is coupled, via the consequential microscopic force fluctuations, nonlinearly to concentration fluctuations of all spatial scales. Alternative closures to Eq. (18) have been explored [5,7]. However, in order to reproduce all the qualitative features of the observed spectra of dense supercooled fluids the closure of the generalized Langevin equation must contain terms that are at least quadratic in different correlation functions, e.g., the correlation of concentration fluctuations of different wave vectors as in Eq. (18). By increasing the coupling through *continuously* varying the static properties (such as the static structure factor appropriate to the concentration of the metastable fluid) a dynamic instability is crossed, at a concentration ϕ_c, beyond which the fluid structure is partially arrested. The approach to the transition from the fluid side is accompanied by the emergence of two distinct relaxation processes, the α and β processes, whose time scales τ_α and τ_β diverge algebraically with nonuniversal exponents. The slower α process freezes in at the transition while the faster β process persists into the nonergodic glass.

Close to the transition the theory makes general but detailed predictions for the particle dynamics. For intermediate times $\tau_\alpha \gg \tau \gg \tau_0$, where τ_0 characterizes the time scale of the local or microscopic particle motion (or atomic vibrations), the dynamics are governed by the β process for which the predicted ISF has the form

$$f(q,\tau)=f_c(q)+h(q)c_\epsilon g_\pm(\tau/\tau_\beta) , \qquad (19)$$

where $f_c(q)$, referred to as the critical nonergodicity parameter, represents the fraction of the structure that is arrested at the concentration ϕ_c. The amplitude of the β process is $h(q)c_\epsilon$, with $c_\epsilon = |\epsilon|^{1/2}$, and $g_\pm$ is a universal master function for which the $\pm$ subscript indicates the sign of the separation parameter ϵ defined by

$$\epsilon = c_0(\phi - \phi_c)/\phi_c \qquad (20)$$

(c_0 is a material-dependent constant). The scaling time of the β process increases critically with ϵ,

$$\tau_\beta = \tau_0/|\epsilon|^{1/2a} . \qquad (21)$$

In addition, the following limiting results are predicted:

$$g_\pm(\tau \ll 1)=\tau^{-a} , \qquad (22a)$$

$$g_+(\tau \gg 1)=(1-\lambda)^{-1/2} , \qquad (22b)$$

$$g_-(\tau \gg 1)=-B\tau^b , \qquad (22c)$$

where $B > 0$, and the exponents a and b, whose values lie in the ranges $0 < a < 1/2$ and $0 < b < 1$, are specified by the exponent parameter λ. Equation (22a) indicates that during the early part of the β process the dynamics in the fluid ($\epsilon < 0$) and glass ($\epsilon > 0$) are identical. At long times correlation functions saturate in the glass [Eq. (22b)] but decay algebraically in the fluid [Eq. (22c)]. On the macroscopic time scale $\tau \simeq \tau_\alpha$ the dynamics on the fluid side of the transition are governed by the α process for which the theory predicts another scaling law

$$f(q,\tau)=f_c(q)G(q,\tau/\tau_\alpha) . \qquad (23)$$

The scaling time (which varies in proportion to the viscosity) for this slower process is

$$\tau_\alpha = \tau_0/|\epsilon|^\gamma, \quad \gamma = 1/2a + 1/2b . \qquad (24)$$

This paper is concerned with the particle dynamics in the glass phase where, according to the theory, the α process is arrested and only the β process is relevant.

The quoted equations are asymptotic results of mode-coupling theory valid to order $|\epsilon|^{1/2}$. In this regime the dependence on the microscopic frequency is lost; in the generalized Langevin equation the microscopic frequency is the only term that distinguishes the ballistic dynamics of atoms from the diffusive dynamics of suspended particles. To this extent the above results are universal, i.e., they are independent of the nature of the material and its thermal history. Details of the material, as specified by the interaction potential, enter the theory implicitly via the static structure factor $S(q)=F(q,0)$ from which the vertex function $V(q;q',q'')$ can be calculated [7,8]. This specifies the parameter λ which, in turn, determines the functions $g_\pm$ and the exponents a and b. Detailed solution of the mode-coupling equations therefore, has only been accomplished so far for simple systems, such as the hard-sphere fluid [6,33,34], for which $S(q)$ is known. The critical concentration predicted for the hard-sphere system is $\phi_c = 0.52$ which, as we shall see below, is somewhat lower than the experimental glass transition concentration for hard-sphere colloids. For later reference we mention that, in addition to the asymptotic results for hard spheres, Bengtzelius, Götze, and Sjölander [6] and more recently Fuchs et al. [24] obtained explicit results for the nonergodicity parameters, $f(q, \infty)$, for hard-sphere glasses for a range of values of ϵ.

We mention two further aspects that are relevant particularly when drawing comparisons between mode-coupling theory and experiment. First, the above results, apply only to the slow dynamic processes that emerge at long times in very dense fluids in the vicinity of the glass transition. The time scales of these processes lie well beyond the microscopic time, τ_0, characteristic of atomic vibrations or small-scale diffusive motions of suspended particles. The time τ_0 is, in principle, the only parameter in the theory; it connects the mathematical and experimental time scales. Second, the sharp transition outlined above is predicted by the theory when the coupling of concentration fluctuations to particle currents is neglected. Its inclusion, to allow for the hopping motions that result from collective excitations, rounds or obscures the

sharp transition [35]. Since colloidal particles exchange energy and momentum only with the suspending liquid such hopping motions are likely to be significantly suppressed in colloidal glasses.

III. EXPERIMENTAL DETAILS

A. Sample preparation

The particle suspensions used in this work are similar to those described in a number of earlier studies [1–3,20,30,36]. The particles comprise a poly-(methylmethacrylate) (PMMA) core coated with a chemically grafted layer of poly-(12-hydroxystearic acid) (PHSA) of approximately 10 nm thickness. Two preparations were used; their hydrodynamic radii, R_H, and polydispersities (or coefficient of variation of the particle size distribution) measured by DLS [37] on dilute samples are listed in Table I. Concentrated suspensions of these particles, of refractive index $n \simeq 1.5$, in a hydrocarbon liquid, such as decalin ($n \simeq 1.48$), are opaque and basically unsuitable for light scattering studies. However, the addition of a high refractive index liquid, carbon disulfide ($n \simeq 1.63$) in this case, gives control over the turbidity and provides samples that, at least in the region of the main maximum of the static structure factor, give ample single but negligible multiple scattering of light. Following this optical matching procedure, suspensions were brought to the required concentration by centrifugation of the samples, removal of an appropriate weight of supernatant, careful sealing to minimize solvent evaporation, and gentle tumbling for about 1 day to redisperse the compact sediment. Each sample was prepared in an optical cuvette (of 1-cm square cross section) and comprised approximately 2 cm^3 of suspension in which the weight fraction of particles was known to an accuracy of about 0.2%. From this the fractional volume, ξ, of the "particle cores" was calculated using literature values for the densities of the respective components.

B. Light scattering

The DLS measurements were performed with conventional equipment which consisted of a home-built goniometer, comprising a temperature controlled sample holder and a horizontally rotating detector assembly. A Spectra Physics 165 Kr$^+$-ion laser, operated at the wavelength $\lambda = 647.1$ nm, was sharply focused in the sample (focal waist about 100 μm). This optical equipment was mounted on a mechanically isolated platform to ensure long-term alignment. The latter, along with the intensity and beam-pointing stability of the laser were checked periodically by measuring the zero-time value or "intercept," $g_T^{(2)}(q,0)$, of the light scattering from a piece of frosted glass for a duration of $T = 1000$ s; values obtained were typically $g_T^{(2)}(q,0) \lesssim 1.003$. In most cases the normalized, time-averaged, intensity correlation functions, $g_T^{(2)}(q,\tau)$, were calculated from the digitized photon signal with Brookhaven Instruments BI2030 and BI8000 correlators. To capture the broad range of dynamic processes in very concentrated metastable fluid and glass phases these two correlators were operated in parallel in a manner to ensure that each received the same photon signal. Optimum selection of the sample times and channel spacing gave a combined dynamic range of just over 6 decades. In some of the most recent measurements reported here we employed an ALV5000 correlator with 256 logarithmically spaced channels that span delay times from 0.2 μs to 3000 s.

The derivation of Eq. (11) assumes a point detector which, as stated above, means that for an ergodic sample $g_T^{(2)}(q,0) = 2$. In practice this requires a detector aperture much smaller than one coherence area or speckle. This was achieved by reducing the detector aperture until for an ergodic sample (e.g., a suspension in an equilibrium fluid phase) $g_T^{(2)}(q,0) = 1.98 \pm 0.02$. Thus, for this arrangement the constant c appearing in Eq. (3) is $c = 0.98$. The arrest of concentration fluctuations, i.e., the nonergodicity of the sample on the time scale T of the experiment, is evident in DLS by a measured value for $g_T^{(2)}(q,0)$ of less than 2. Intercepts were obtained from the measured intensity autocorrelation functions, $g_T^{(2)}(q,\tau)$, by the usual cumulant analysis [38].

The other two quantities appearing in the right-hand side of Eq. (11), required for the evaluation of the ISF from $g_T^{(2)}(q,\tau)$, are the time-averaged intensity, I_T, and the ensemble-averaged intensity, I_E. I_T is simply given by the average number of photon detections accumulated by the correlator during a particular measurement. I_E was determined from the photon counts accumulated while the sample was moved vertically in the laser beam by a computer-controlled motor. About 15 such scans through different parts of the sample ensured that estimates of I_E, based on at least 2000 independent speckles in this procedure, were accurate to about 1%.

IV. RESULTS AND DISCUSSION

A. Visual behavior of the samples

Previous work [1,39] on suspensions of similar particles has already described in detail the overall phase behavior and its resemblance to that of the ideal hard-sphere sys-

TABLE I. Designation of latices, hydrodynamic radius R_H, polydispersity, effective hard-sphere radius R, and glass transition volume fraction ϕ_G. Results shown in all figures, except Fig. 2, are based on samples prepared from latex 1. Figure 2 is based on data from latex 2.

Latex	R_H (nm)	Polydispersity (%)	R (nm)	ϕ_G
1 (SMU 21)	210±3	3–5	206	0.563±0.001
2 (SMU 29)	205±3	3–5	199	0.570±0.002

tem. For completeness we give a brief description here. Samples prepared by the above procedures and left undisturbed after tumbling showed the following behavior with increasing concentration: They remained as colloidal fluid, separated into coexisting crystalline and fluid phases, or became fully crystalline. The crystallization in these cases was by homogeneous nucleation, evidenced by the appearance of small Bragg-reflecting crystals that were homogeneously distributed throughout the sample. The crystals were easily shear melted by simply tumbling the samples, thus providing suspensions in their metastable fluid states. Recrystallization was usually evident in less than about half an hour of being left undisturbed. In the samples between the freezing and melting concentrations the crystals settled gravitationally and a distinct boundary, separating the coexisting polycrystalline and fluid phases, was evident after several days. Using a procedure similar to that described by Paulin and Ackerson [15] the effect of slow gravitational settling of the particles was eliminated. The "gravity-free" proportion of crystalline phase plotted as a function of sample concentration gave a straight line (lever rule). Extrapolation to 0% crystal yielded the core volume fraction, ξ_F, of the suspension at freezing. The concentrations of all samples prepared from a particular stock suspension of particles were then expressed as effective hard-sphere volume fractions, as

$$\phi = \xi \phi_F / \xi_F , \tag{25}$$

where $\phi_F = 0.494$ is the freezing volume fraction of the hard-sphere fluid, known from computer simulation [40], and ξ is the volume fraction of particle cores. This procedure gave an effective hard-sphere melting volume fraction of $\phi_M = 0.542 \pm 0.003$, in good agreement with the value of 0.545 ± 0.002 established by computer simulation for the melting concentration of the hard-sphere crystal [40]. This result, which has been reproduced for several suspensions of PMMA particles of different radii [16], is a strong indication that the interaction between these particles is very similar to that of hard spheres.

The static structure factors, $S(q)$, measured on these suspensions [3] can be scaled so that they fit the Percus-Yevick result, with the empirical correction of Verlet and Weis [41], for the hard-sphere fluid, at least in the region of the position, q_m, of the primary maximum. We use the same procedure as detailed elsewhere [3,42] to locate q_m for a suspension at the freezing concentration. The effective hard-sphere radius, R, of the particles in the refractive index matched suspensions is given by

$$R = Q_m / q_m , \tag{26}$$

where $Q_m = 3.47$ is the theoretical value [41] of the position of the main maximum of $S(q)$ in units of the hard-sphere radius. The values of R obtained for the two suspensions used in this work are listed in Table I. Henceforth scattering vectors are expressed in units of the reciprocal of the hard-sphere radius, i.e., as qR.

Beyond ϕ_M a volume fraction ϕ_G was reached where homogeneously nucleated crystallization was superseded by the slow formation of larger crystals, nucleated heterogeneously at the meniscus, walls of the optical cuvette, or possibly on the occasional impurity. These larger crystals were evident after several hours at volume fractions just above ϕ_G but their formation slowed significantly at higher volume fractions. On approaching the random close-packing volume fraction, $\phi = 0.64$, progressively smaller proportions of crystal grew from the menisci over increasingly long periods (days to weeks) while the rest of the sample remained amorphous. Here we identify ϕ_G as the glass transition volume fraction and all DLS results discussed in the following subsections apply to the glass phase $(\phi > \phi_G)$. We attribute the small variations in the value of ϕ_G $(0.555-0.575)$ observed here (see Table I) and in previous work [1,3] to differences in the polydispersities, that are too small to detect by DLS [37], and also to the systematic error in the effective hard-sphere volume fraction incurred in the determination of ξ_F for different suspension preparations. However, for a particular preparation the concentrations, scaled according to Eq. (25), are internally consistent and accurate to about 0.5%.

B. Testing of a model for colloidal glasses

In this subsection we present several tests of the validity of Eq. (11) which expresses the (ensemble-averaged) ISF in terms of a single measurement of the time-averaged intensity correlation function of a nonergodic medium. The basic assumption in the derivation of Eq. (11), as well as its corollary equation (12), is that the particles are effectively localized about fixed average positions for the duration of the experiment. The extent to which a colloidal glass shows this property can be tested by making measurements of different duration T and, in each case, calculating the apparent nonergodicity param-
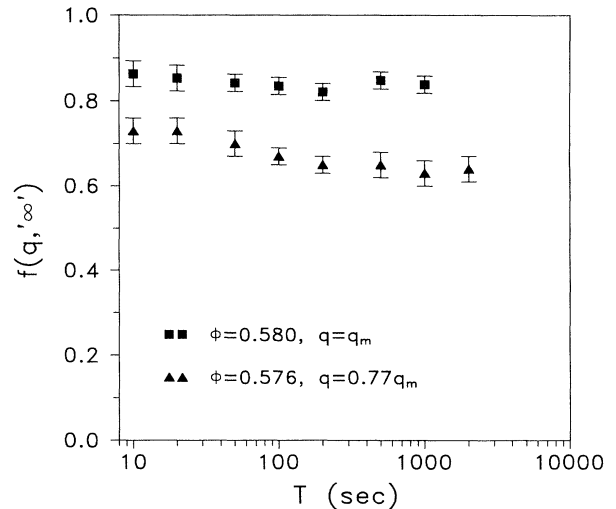

FIG. 1. Apparent nonergodicity parameters $f(q, \text{"}\infty\text{"})$ of colloidal glasses as a function of the duration T of the measurement. Squares signify the sample volume fraction $\phi = 0.580$, measurements made at the scattering vector (multiplied by the hard-sphere radius) of $qR = 3.35$ (i.e., near the position of the main peak in the static structure factor). Triangles denote the sample at $\phi = 0.576$ and $qR = 2.77$.

eter $f(q, ``\infty")$ from the measured values of $g_T^{(2)}(q,0)$, I_T, and I_E by use of Eq. (12). Figure 1 shows the results of such measurements, for T ranging from 10 to 2000 s, for two colloidal glasses at volume fractions $\phi=0.576$ and 0.580. Each data point was obtained by averaging about ten measurements of $f(q, ``\infty")$. Between each of these measurements the sample was moved relative to the laser beam so that a different volume was illuminated, resulting in a different value of the time-averaged (or speckle)
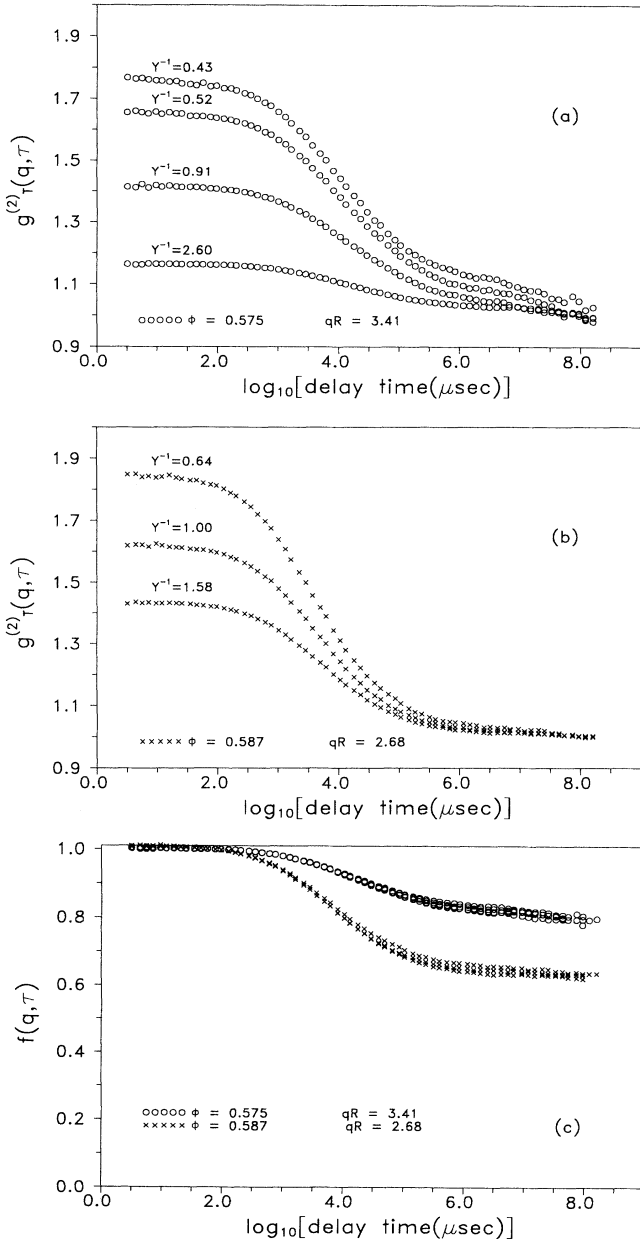
intensity I_T. It can be seen that $f(q, ``\infty")$ decreases with increasing $T$ up to $T \simeq 100$ s, implying the existence of residual "fast" fluctuations on this time scale associated with the local motions of the particles about their fixed average positions. However, for $100 \lesssim T \lesssim 2000$ s, $f(q, ``\infty")$ is essentially independent of T. At the very least, this behavior demonstrates the existence of fluctuations with a bimodal distribution of relaxation times; fast fluctuations, with relaxation times of less than 100 s, and slow fluctuations, associated with large-scale "structural" relaxations whose time scales greatly exceed 2000 s. Thus concentration fluctuations, due to large-scale particle motions, are effectively arrested on any reasonable experimental time scale, i.e., the particles are localized, as assumed in the model for a nonergodic medium [21].

Next we examine time-averaged intensity correlation functions for several colloidal glasses obtained by measurements of $T = 1000$ s duration. As above, the sample was moved relative to the laser beam between each measurement. The data in Fig. 2 show that very different results are obtained for $g_T^{(2)}(q,\tau)$ for different values of I_T (or $Y = I_E/I_T$) corresponding to different volumes in the sample. The results of individual 1000-s measurements, shown here, exhibit some statistical noise as well as evidence of residual fast fluctuations that persist to times of order 100 s (see Fig. 1). This is more noticeable in Fig. 2(a) for the volume fraction, $\phi=0.575$ ($\epsilon \simeq 0.01$), which, for this latex (latex 2) is only marginally inside the glass phase ($\phi_G=0.570\pm0.002$). Increasing ϕ results in arrest of a progressively larger fraction of the concentration fluctuations and the "compression" of the nonarrested fluctuations to shorter times. Figure 2(c) shows the ISF's calculated, with Eq. (11), from the data in Figs. 2(a) and 2(b). Significantly, the same ISF is obtained for the different time-averaged intensity autocorrelation func-
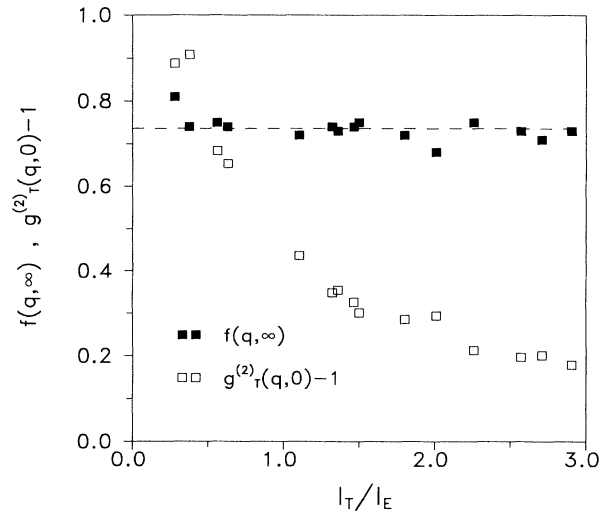

FIG. 2. (a), (b) Normalized intensity autocorrelation functions, $g^{(2)}T(q,\tau)$, time-averaged over $T = 1000$ s as functions of the delay time for the indicated speckle intensities I_T/I_E ($= Y^{-1}$), volume fractions and scattering vectors. (c) Intermediate scattering functions, $f(q,\tau)$, derived from the above using Eq. (11).

FIG. 3. Verification of Eq. (12). Measured values of the mean-squared intensity fluctuation, $g^{(2)}_T(q,0)-1$ (open squares) and derived values of the nonergodicity parameters, $f(q,\infty)$ (solid squares) are plotted against I_T/I_E for a range of speckle intensities I_T. The dashed line shows the average value of $f(q,\infty)$. Measurements are made for $\phi=0.594$ and $qR =2.77$.
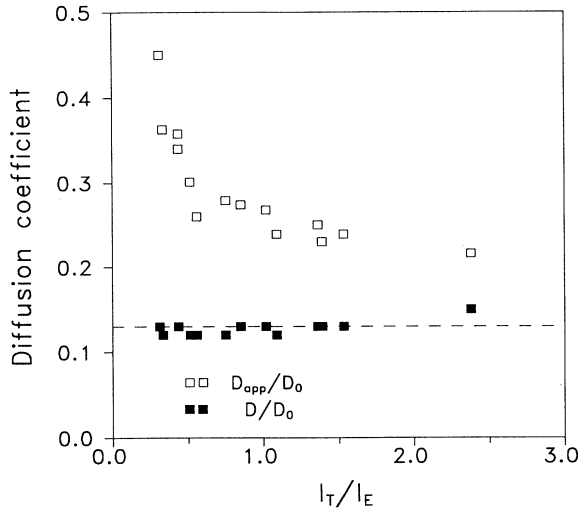
FIG. 4. Apparent diffusion coefficient, D_{app}/D_0 (open squares), obtained from the initial decay of the time-averaged intensity autocorrelation function [Eq. (13)] and the correct diffusion coefficient, D/D_0 (solid squares) in units of the free-particle diffusion coefficient, D_0, calculated from the intermediate scattering function [Eq. (14) or (15)] are plotted against I_T/I_E; sample at $\phi=0.579$ and $qR=4.23$. The dashed line shows the average value of D/D_0.

tions. This supports the main result of Sec. II A and Ref. [21] that the ensemble-averaged ISF, calculated for a colloidal glass from Eq. (11), is a property of the sample independent of the particular scattering volume.

Figure 3 illustrates that, for a colloidal glass, the mean-squared intensity fluctuation, $\sigma^2=g_T^{(2)}(q,0)-1$, decreases with increasing time-averaged intensity, I_T. However, while different values of $g_T^{(2)}(q,0)$ are recorded for different speckle intensities I_T, corresponding to different scattering volumes in the sample, Eq. (12) gives essentially the same value for $f(q,\infty)$. Also, as shown in Fig. 4, the apparent diffusion coefficient, D_{app}, calculated from Eq. (13) varies with I_T and significantly overestimates the correct short-time diffusion coefficient D, obtained from Eq. (15).

The results of Figs. 2–4 demonstrate that for colloidal glasses the measured time-averaged intensity correlation function is dependent on the choice of the particular scattering volume in the sample. However, the ISF calculated from Eqs. (11) and (12) is an ensemble-averaged property of the sample. We mention that the model for a nonergodic medium and the light scattering theory based on it, as outlined in Sec. II A and detailed in Ref. [21], has also been verified for polymer gels as well as colloidal particles trapped in gels [43].

C. Dynamic-light-scattering results

Having verified both the model and light scattering theory for nonergodic media we examine the intermediate scattering functions measured for colloidal glasses in more detail.

First, the nonergodicity parameters, $f(q,\infty)$, measured

on colloidal glasses (prepared from latex 1, see Table I) are shown in Fig. 5 for concentrations ranging from $\phi_G=0.563$ ($\epsilon\simeq0$) to random close packing, $\phi=0.64$ ($\epsilon\simeq0.14$). Each data point represents an average over several measurements, ranging in duration from 200 to 1000 s, with different values of I_T. In the regions where the coherent scattering is weak (at small q, $qR\lesssim2.5$, where the static structure factor has a small value and large q, $qR\gtrsim5$, near the minimum in the single-particle form factor) multiple scattering may cause uncertainties in the data. In addition, incoherent scattering, associated with the small spread in particle size (see Table I), may contribute at small q. (Single-particle motions, as measured by the incoherent ISF, are much slower than the small wave-vector collective motions, measured by the coherent ISF [20].) However, in the vicinity of the primary maximum of $S(q)$, where (single) coherent scattering is strong the results should be reliable. For reference, the static structure factor calculated from the Percus-Yevick expression for hard spheres at $\phi=0.563$ is also shown in Fig. 5. The increase in $f(q,\infty)$ with particle concentration reflects the increasingly restricted particle motions, culminating in the effective cessation of motion at random close packing where $f(q,\infty)\simeq1$.

As mentioned in the Introduction we find, to the extent that the experimental accuracy in the sample concentration allows, coincidence of the concentration ϕ_G, where homogeneously nucleated crystallization is first suppressed, and that where DLS indicates the partial
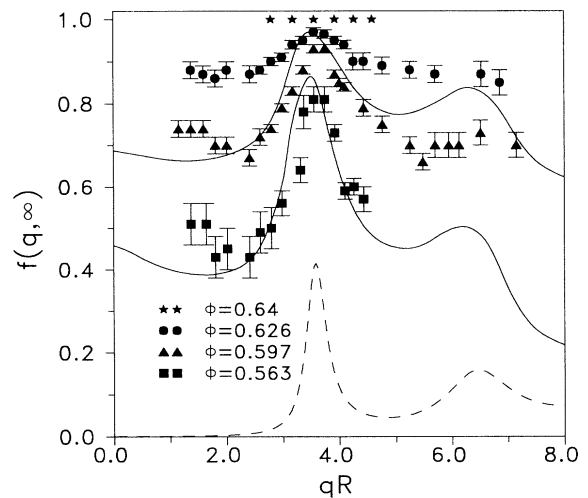

FIG. 5. The nonergodicity parameters $f(q,\infty)$ of hard-sphere colloidal glasses as functions of volume fraction and scattering vector. Experimental data: squares, $\phi=0.563$, separation parameter $\epsilon\simeq0$; triangles, $\phi=0.597$, $\epsilon=0.060$; circles, $\phi=0.626$, $\epsilon=0.114$; stars, random-close-packed sample, $\phi\simeq0.64$, $\epsilon\simeq0.14$. The solid curves are the mode-coupling predictions [6] for the perfect hard-sphere system at separation parameters $\epsilon=0$ (lower curve) and $\epsilon=0.066$ (upper curve). The dashed curve is the Percus-Yevick static structure factor for hard spheres at $\phi=0.563$ reduced in magnitude by a factor of 10.

arrest of concentration fluctuations. We therefore identify ϕ_G with the critical concentration, ϕ_c, where mode-coupling theory predicts structural arrest, i.e., where a nonzero nonergodicity parameter, $f(q, \infty)$, is first found.
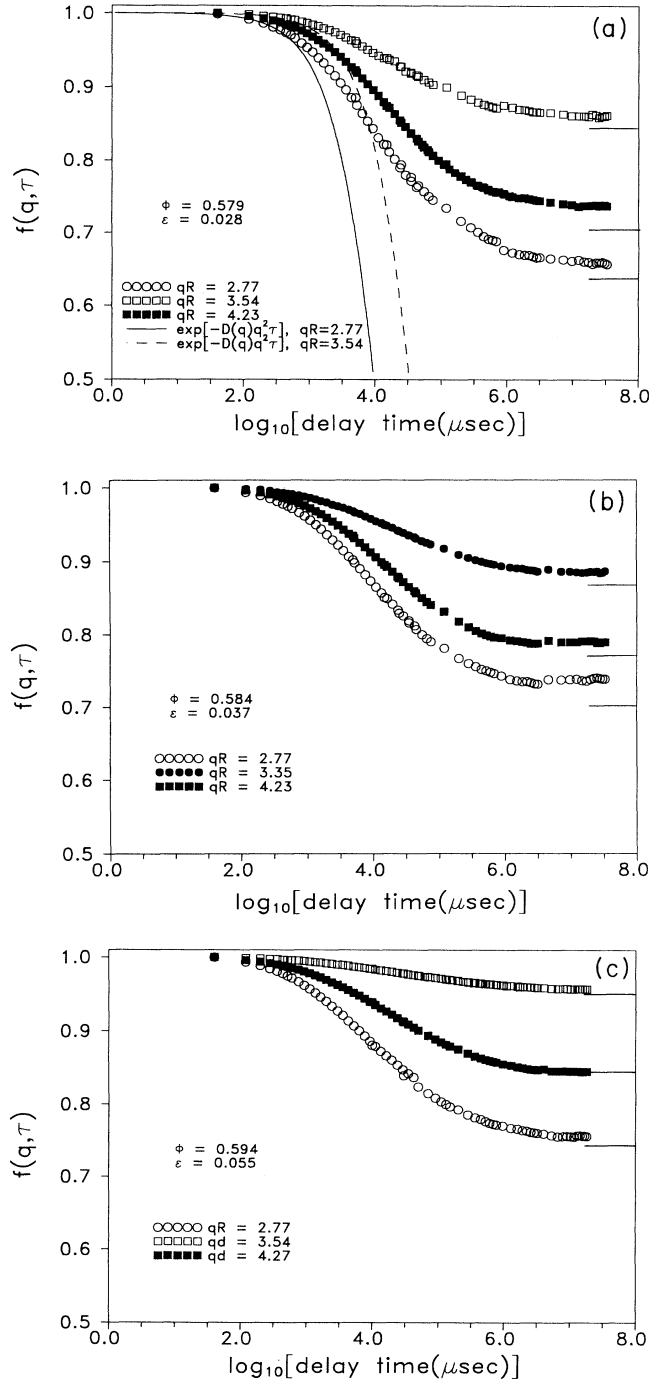

FIG. 6. Normalized intermediate scattering functions vs logarithm of the delay time. Measurements are made on samples at the indicated concentrations and scattering vectors. The small horizontal bars at the right indicate corresponding values of the nonergodicity parameters, $f(q, \infty)$. The solid and dashed lines are calculated from Eq. (14) for $qR = 2.77$ and 3.54.

For the hard-sphere system the theoretical prediction is $\phi_G = 0.52$ [6,33]. Since this value is somewhat smaller than the experimental value of $\phi_G \simeq 0.563$ observed for this suspension (latex 1, see Table I), concentrations are expressed in terms of the experimental separation parameter ϵ [Eq. (20) with $c_0 = 1$] in order to compare experiment with mode-coupling theory. The solid curves in Fig. 5 are the theoretical predictions of Bengtzelius, Götze, and Sjölander [6] at separation parameters $\epsilon = 0$ and 0.066. One sees that these agree rather well with the experimental data for $\epsilon \simeq 0$ and 0.060, although the theory seems to overestimate slightly the maximum values of $f(q, \infty)$. Importantly, there are no parameters involved in this comparison.

Results for the ISF's are displayed in Fig. 6 for colloidal glasses at several concentrations and scattering vectors. To prevent overcrowding the figures only three results are shown for each concentration, at scattering vectors below, near, and above the position of the main peak in the static structure factor. Again, each curve was obtained by averaging over 5–10 measurements, each of 1000 s duration, with different values of I_T. Less than the first 10% of the total decay of the ISF's is accounted for by the microscopic particle motion, given by the quantity $\exp[-D(q)q^2\tau]$. The short-time collective diffusion coefficients, $D(q)$, were calculated from the initial decay of the ISF's [see Eq. (14)] for $\phi = 0.579$ at the scattering vectors indicated in the figure. Beyond this initial decay the relaxation of concentration fluctuations slows significantly until the fluctuations appear essential-
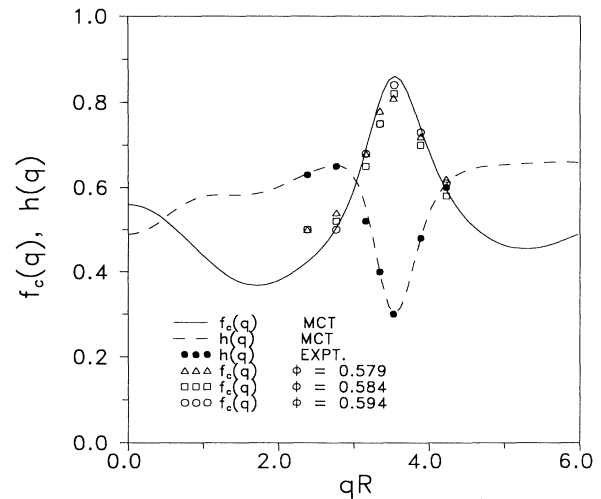

FIG. 7. Critical nonergodicity parameters, $f_c(q)$ (open symbols), and critical amplitudes, $h(q)$ (solid circles), used to convert results of Fig. 6 to scaled results in Fig. 8 according to Eq. (19). The solid and dashed lines are the mode-coupling predictions for $f_c(q)$ and $h(q)$, respectively. The theoretical $f_c(q)$ in this figure calculated by Fuchs *et al.* [34] used the Percus-Yevick and hard-sphere fluid structure factor which incorporated the Verlet-Weis [41] correction. These $f_c(q)$ are slightly different, particularly at small q, from those shown in Fig. 5 obtained by Bengtzelius, Götze, and Sjölander [6], which did not include this correction. In the region where the experimental data are most reliable there is no significant difference between the two results.

ly frozen at $\tau \simeq 1$ s. Except at the highest concentration ($\phi = 0.594$), a slight decay, of a few percent at most, is evident outside the statistical and correlator noise from about 1 to 1000 s. The values of the ISF's at the delay time of 1000 s (the duration of the experiments) are given by the nonergodicity parameters $f(q, \infty)$ and are indicated by the horizontal bars in Fig. 6. In view of our earlier conjecture that phonon-activated processes may be absent in colloidal glasses, we suggest that, given the finite polydispersity of the suspensions (see Table I), this small remnant decay of the ISF's at long times may be associated with a trace concentration of small mobile particles. A genuine extremely slow structural relaxation, other than activated transport, is another possibility.

Next we check whether the ISF's of Fig. 6 comply with the scaling prediction of mode-coupling theory, Eq. (19), for the β process. The theoretical critical nonergodicity parameters, $f_c(q)$, and critical amplitudes, $h(q)$, calculated for the hard-sphere system [34] are shown in Fig. 7. Rather than attempting an alignment of the data for different scattering vectors, at a given concentration, by independently varying both $f_c(q)$ and $h(q)$, we used the theoretical values for $h(q)$ and adjusted $f_c(q)$ to provide the best overlap of the measured intermediate scattering functions at long times. The results of this procedure, applied to the data in Fig. 6, are shown in Fig. 8. Systematic errors, due to correlator noise or poor statistics of the correlation functions close to background, partly masked in this procedure at long times, are moved to the short-time regime. Despite this the expected [30] strong dependence on the scattering vector of the decay at short times, discussed in Sec. II A, is fairly well preserved by the scaling procedure. At long times the results for different scattering vectors scale to a single curve. For the two lower concentrations [Figs. 8(a) and 8(b)] the scaling is obeyed for a dynamic range of almost three decades roughly from the points of inflection ($\log_{10}\tau > 4.5$). Presumably the inflection marks a crossover from the microscopic dynamics to the slower β process. With increasing concentration the q-dependent short-time decay, associated with the small-scale particle motions, extends to longer times. At the highest concentration [Fig. 8(c)] the dynamic range of the scaling property is reduced to less than two decades. However, the separation parameter ($\epsilon \simeq 0.055$) at this concentration is probably too large for the asymptotic results of mode-coupling theory to be entirely applicable [24].

The critical nonergodicity parameters, shown in Fig. 7, obtained in the above scaling are consistent for the three concentrations studied and they are also in good agreement with the theoretical results. Importantly, they agree quantitatively with those measured directly on a sample at the glass transition concentration (see Fig. 5). The wave-vector variation of $f(q)$ (Figs. 5 and 7) is in harmony with the static structure factor. The physical explanation for this behavior is that $S(q)$ is proportional to the mean-squared amplitude, or compressibility, of concentration fluctuations of wave vector q, and it is entirely plausible that the most compressible fluctuations, those of wave vector q_m, should be most strongly arrested at the glass transition. For the same reason, the ampli-

tude of the complementary nonarrested fluctuations, $h(q)$, mirrors $S(q)$.

Furthermore, according to mode-coupling theory the scaled intermediate scattering functions are given by $[f(q,\tau) - f_c(q)]/h(q) = c_\epsilon g_+(\tau/\tau_\beta)$ [see Eq. (19)]. Thus,
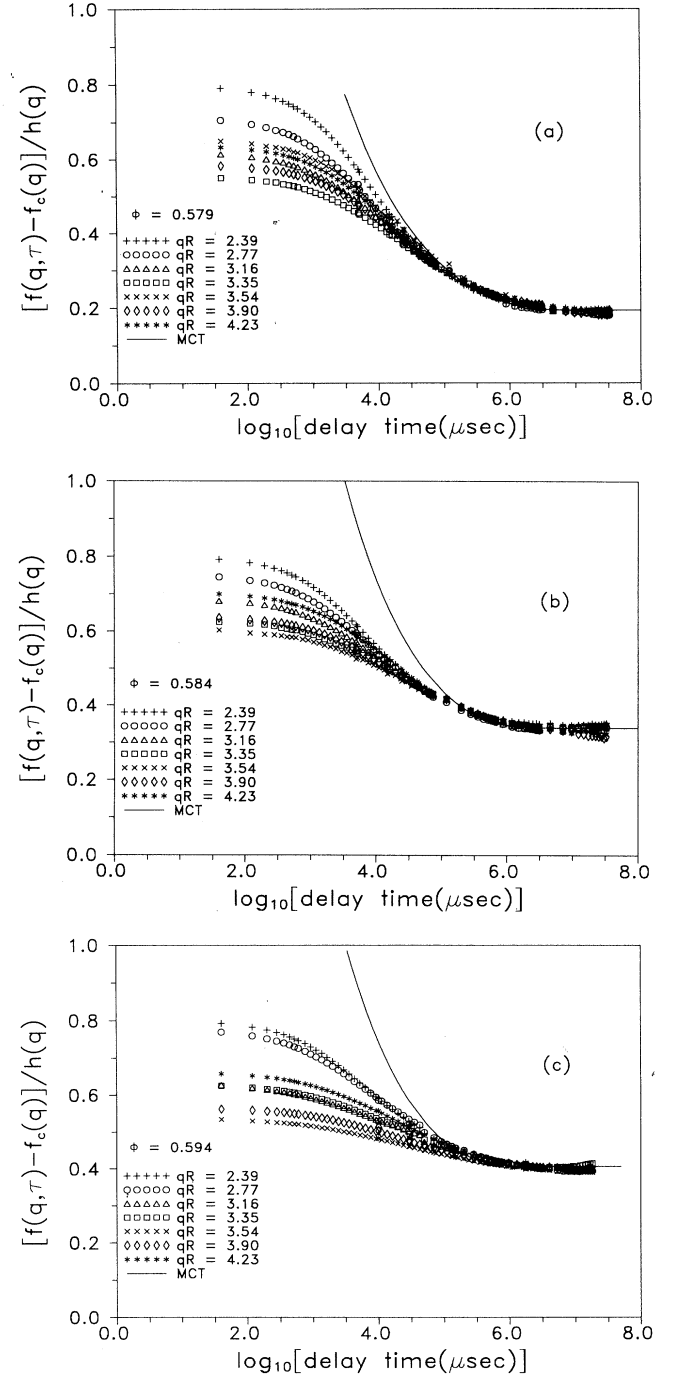

FIG. 8. Intermediate scattering functions scaled according to Eq. (19). Thus $f[(q,\tau) - f_c(q)]/h(q)$ is plotted as function of the logarithm of the delay time. The critical nonergodicity parameters, $f_c(q)$, and critical amplitudes, $h(q)$, required to obtain the overlap at long times, are shown in Fig. 7. The solid curve is the mode-coupling master function, $g_+(\tau)$, for the β process in the hard-sphere glass.
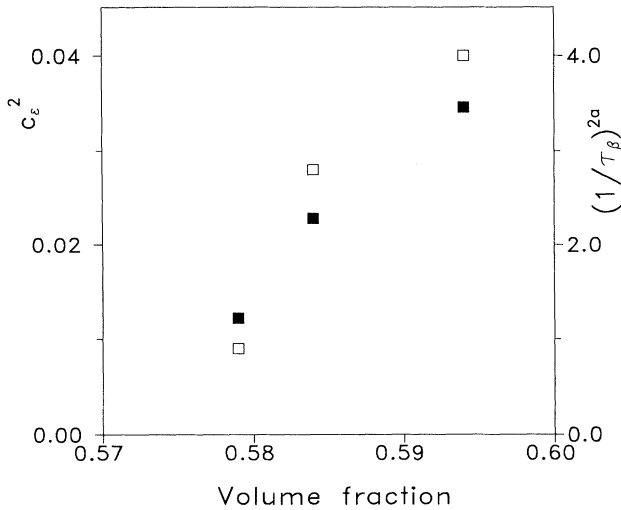
FIG. 9. The correlation scale c_ϵ and the scaling time τ_β, of the β process; c_ϵ^2 (open squares) and $(1/\tau_\beta)^{2a}$ (solid squares) vs volume fraction.

the correlation scale c_ϵ and the scaling time τ_β were adjusted to fit the predicted master function $g_+(\tau/\tau_\beta)$ of the β process to the scaled data of Fig. 8. One sees that it is possible to align the master function with the data roughly from the time $[\log_{10}\tau > 4.5$ in Figs. 8(a) and 8(b)] where the scaling applies. Again, for reasons suggested above, the region of agreement is less extensive at the highest concentration [Fig. 8(c)].

In order to check the predicted algebraic dependence of τ_β on ϵ [Eq. (21)] and the square-root dependence of c_ϵ on ϵ we plot, in Fig. 9, $(1/\tau_\beta)^{2a}$ and c_ϵ^2 as functions of volume fraction (for hard spheres $a = 0.301$). The concentration dependence of both the experimental scaling time and the correlation scale are consistent with the theory. The result for τ_β in particular verifies the surprising prediction that the time scale of the β process decreases as one goes deeper into the glass. The narrow range of volume fractions in the hard-sphere glass where the asymptotic results of mode-coupling theory are expected to be accurate [24], along with the errors that accrue in the above manipulation of the data, preclude quantitative tests of these scaling predictions. Linear extrapolation of the two sets of results in Fig. 9 to zero give ϕ_c in the range 0.565–0.575, which is at least compatible with the more direct estimates of the glass transition concentration (see Table I).

V. SUMMARY AND CONCLUSIONS

Colloidal suspensions of near-micrometer-sized PMMA particles stabilized by thin adsorbed layers of PHSA show the equilibrium phase behavior as well as a glass transition consistent with those seen in computer simulations for perfect hard spheres [40,44]. A glass transition concentration is identified where homogene-

ously nucleated crystallization is superseded by a much slower crystallization nucleated heterogeneously at surfaces. One might speculate whether in the absence of surfaces heterogeneous crystallization would proceed at all and samples at $\phi > \phi_G$ would remain amorphous indefinitely. Nevertheless, studies on several different suspensions of PMMA particles consistently show a close correspondence of the concentration of this observed glass transition and that where the time scale of the slowest concentration fluctuations significantly exceeds the duration of a 1000-s experiment, i.e., suppression of crystallization and cessation of large-scale particle diffusion occur at essentially the same concentration.

Determination of the intermediate scattering functions of colloidal glasses by dynamic light scattering requires a procedure that properly averages over both the fluctuating and the arrested structure. The results of Sec. IV B show that disregarding the nonergodicity of the scattering medium leads to incorrect interpretations of DLS results. In this paper we have verified the theory of DLS based on a model for a nonergodic medium which assumes that the particles are localized about an amorphous distribution of fixed average positions. The statistical properties of the light scattered by the fluctuating structure are the same for all scattering volumes in the sample and, therefore, can be unambiguously obtained in a single time average. However, the distribution of fixed average positions, i.e., the arrested structure, is different for different scattering volumes. Thus, a single measurement of the time-averaged intensity autocorrelation function plus the ensemble-averaged intensity are required to compute the (ensemble-averaged) intermediate scattering function. Verification of this theory of DLS by colloidal glasses was achieved by demonstrating that, while the time-averaged intensities and intensity autocorrelation functions vary markedly over different scattering volumes in the sample, the calculated intermediate scattering functions are invariant.

The nonergodicity parameters were obtained for colloidal glasses at several concentrations over a range of scattering vectors around the position, q_m, of the first maximum in the static structure factor. The results are in good agreement with mode-coupling theory. By expressing the concentrations in terms of the separation parameter ϵ, the comparison in Fig. 5 involved no adjustable parameters.

The intermediate scattering functions are compatible with the scaling predictions for the β process and in agreement with the master function, predicted for the hard-sphere glass, for times beyond those of the microscopic dynamics. Presumably due to the overlap of the small-scale local particle motions with the slower motions described by the β process there was no evidence of the predicted critical decay [given by Eq. (22a)]. Nonetheless, the results confirm that one can separate from the microscopic motion a slower relaxation process for which the spatial and temporal variations are uncorrelated. Near the glass transition the intermediate scattering functions show this factorization property for nearly three decades in time. In this regard the results in this paper are considerably more conclusive than those of pre-

vious neutron scattering experiments on ionic systems [45] and computer simulations on mixtures [46,47]. There the factorization property was demonstrated over a dynamic range of about one decade. Additional significant results of the scaling of the experimental data are that (i) the required nonergodicity parameters and critical amplitudes are in quantitative agreement with mode-coupling theory, (ii) the nonergodicity parameters agree quantitatively with those measured independently at the estimated glass transition concentration, and (iii) the concentration dependence of both the correlation scale and the scaling time of the β process are compatible with the theory.

In view of the comparisons between experiments on suspensions and mode-coupling theory that have been made in this and previous works [3,8,23–25] some comment is warranted on the hydrodynamic interactions among the suspended particles. Their effect on the dynamics may be exposed most simply, although not completely, by considering the short-time form of the ISF expressed in Eqs. (16) and (17). We argued in Sec. II A that, although the hydrodynamic interactions cause some smearing of the wave-vector dependence of the ISF's, the ISF's still vary strongly with wave vector at short times. As seen in Fig. 8, this variation survives the scaling process. Of course, mode-coupling theory is only concerned with the slow structural relaxation processes that emerge at very high concentrations and it makes no predictions with regard to the microscopic dynamics. However, the strong coupling of the small-scale particle motion, via the hydrodynamic interactions, to the structure leads to a lengthening of the microscopic time scale. This may be the reason for the apparent overlap of the microscopic dynamics with the slower motions described by the β process and the absence of the algebraic time dependence that is predicted for the early part of the β process. In contrast, the time scale of atomic vibrations is relatively insensitive to density or temperature. This is seen quite clearly, for example, in the recent work of Li et al., [48] who measured the susceptibility spectrum of an ionic glass former. There, in addition to the temperature-insensitive phonon peak, an algebraic variation of the susceptibility with frequency was observed in the super-cooled ionic systems for about one decade on both sides of the glass transition temperature. Notwithstanding the

strong wave-vector dependence of the decay rates of the coherent ISF's in colloidal glasses over time scales that lengthen with increasing concentration, the results of Figs. 7 and 8 suggest that the β process eventually emerges and that this process is independent of the nature of the microscopic motions.

Finally we comment on the difference between the glass transition concentration observed in these hard-sphere suspensions and that predicted by mode-coupling theory. There is some variation in the glass transition concentration, $\phi_G = 0.555 - 0.575$, found for different suspension preparations in this and other work [1–3]. We attribute this mainly to systematic errors incurred in the estimation of the factor, based on the freezing concentration, used to convert sample weight fractions to effective hard-sphere volume fractions (see Sec. IV A). The present work, based on more accurate sample preparations, favors larger values in the stated range for ϕ_G. This glass transition concentration is consistent with that ($\phi_G = 0.58 \pm 0.02$) found in computer simulations of the hard-sphere systems [44]. It has been suggested [8,33] that the lower value, $\phi_G = 0.52$, predicted for the glass transition concentration by mode-coupling theory is due to the neglect of hopping motions in the idealized version of theory. This is also the reason suggested for the slightly larger values for the critical nonergodicity parameters relative to experiment (Fig. 5). Considering the difficulties and uncertainties in measurements at the glass transition, we cannot regard these differences in $f_c(q)$ as very significant. However, the difference between the experimental and theoretical values of ϕ_G may be more significant and, if hopping motions are suppressed in colloidal systems, we wonder whether there may be another explanation for the low theoretical value for ϕ_G.

ACKNOWLEDGMENTS

---

*Present address: ICI Australia, Ascot Vale, Victoria 3032, Australia.

[1] P. N. Pusey and W. van Megen, Nature (London) 320, 340 (1986).

[2] P. N. Pusey and W. van Megen, Phys. Rev. Lett. 59, 2083 (1987).

[3] W. van Megen and P. N. Pusey, Phys. Rev. A 43, 5429 (1991).

[4] J. P. Hansen, Phys. World, No. 12, 32 (1991).

[5] E. Leuthuesser, Phys. Rev. A 29, 2765 (1984).

[6] U. Bengtzelius, W. Götze, and A. Sjölander, J. Phys. C 17, 5915 (1984).

[7] W. Götze, in Liquids, Freezing and the Glass Transition, Les Houches Summer School Proceedings Session 51, edit-

ed by D. Lesvesque, J. P. Hansen, and J. Zinn-Justin (North-Holland, Amsterdam, 1981).

[8] W. Götze and L. Sjögren, Rep. Prog. Phys. 55, 241 (1992).

[9] C. A. Angell, J. Phys. Chem. Solids 49, 863 (1988).

[10] F. Mezei, W. Knaak, and B. Farago, Phys. Rev. Lett. 58, 571 (1987); N. J. Toa, G. Li, and H. Z. Cummins, ibid. 66, 1334 (1991).

[11] D. Richter, R. Zorn, B. Frick, and B. Farago, Ber. Bunsenges. Phys. Chem. 95, 1111 (1991).

[12] W. Petry, E. Bartsch, F. Fujara, M. Kiebel, H. Sillescu, and B. Farago, Z. Phys. B 83, 175 (1991).

[13] F. Mezei, Ber. Bunsenges. Phys. Chem. 95, 1118 (1991).

[14] H. Löwen, J. P. Hansen, and J. N. Roux, Phys. Rev. A 44, 1169 (1991).

[15] S. E. Paulin and B. J. Ackerson, Phys. Rev. Lett. **64**, 2663 (1990).

[16] S. M. Underwood, J. R. Taylor, and W. Van Megen (unpublished).

[17] B. J. Berne and R. Pecora, *Dynamic Light Scattering* (Wiley, New York, 1976).

[18] E. Bartsch, O. Debus, F. Fujara, M. Kiebel, W. Petry, and H. Sillescu, Ber. Bunsenges. Phys. Chem. **95**, 1146 (1991).

[19] F. Mezei, in *Liquids, Freezing and the Glass Transition* (Ref. [7]).

[20] W. van Megen and S. M. Underwood, J. Chem. Phys. **91**, 552 (1989); Langmuir **6**, 35 (1990).

[21] P. N. Pusey and W. van Megen, Physica A **157**, 705 (1989).

[22] P. N. Pusey, in *Photon Correlation Spectroscopy and Velocimetry*, edited by H. Z. Cummins and E. R. Pike (Plenum, New York, 1977).

[23] W. Götze and L. Sjögren, Phys. Rev. A **43**, 5442 (1991).

[24] M. Fuchs, W. Götze, S. Hildebrand, and A. Latz, Z. Phys. B **87**, 43 (1992).

[25] W. van Megen, S. M. Underwood, and P. N. Pusey, Phys. Rev. Lett. **67**, 1586 (1991).

[26] P. N. Pusey, in *Liquids, Freezing and the Glass Transition* (Ref. [7]).

[27] C. W. J. Beenakker and P. Mazur, Physica A **126**, 349 (1984).

[28] P. N. Pusey, J. Phys. A **8**, 1433 (1975).

[29] P. G. de Gennes, Physica **25**, 825 (1959).

[30] W. van Megen, R. H. Ottewill, S. M. Owens, and P. N. Pusey, J. Chem. Phys. **82**, 508 (1985).

[31] J. P. Hansen and I. R. McDonald, *Theory of Simple Liquids* (Academic, London, 1986).

[32] B. J. Ackerson, J. Chem. Phys. **69**, 684 (1978).

[33] J-L. Barrat, W. Götze, and A. Latz, J. Phys. Condens. Matter **1**, 7163 (1989).

[34] M. Fuchs, I. Hofacker, and A. Latz, Phys. Rev. A **45**, 898 (1992).

[35] W. Götze and L. Sjögren, Z. Phys. B **65**, 415 (1987).

[36] P. N. Pusey and W. van Megen, J. Phys. (Paris) **44**, 285 (1983).

[37] P. N. Pusey and W. van Megen, J. Chem. Phys. **80**, 3513 (1984).

[38] D. E. Koppel, J. Chem. Phys. **57**, 4814 (1972); J. C. Brown, P. N. Pusey, and R. Dietz, *ibid.* **62**, 1136 (1975).

[39] W. van Megen, P. N. Pusey, and P. Bartlett, Phase Transitions **21**, 207 (1990).

[40] W. G. Hoover and F. H. Ree, J. Chem. Phys. **49**, 3609 (1968).

[41] L. Verlet and J. J. Weis, Phys. Rev. A **5**, 939 (1972).

[42] P. N. Pusey, W. van Megen, P. Bartlett, B. J. Ackerson, J. G. Rarity, and S. M. Underwood, Phys. Rev. Lett. **63**, 2753 (1989).

[43] J. G. H. Joosten, E. T. F. Gelade, and P. N. Pusey, Phys. Rev. A **42**, 2161 (1990); J. G. H. Joosten, J. L. McCarthy and P. N. Pusey, Macromolecules **24**, 6690 (1991).

[44] L. V. Woodcock, Ann. N.Y. Acad. Sci. **37**, 274 (1981).

[45] W. Knaak, F. Mezei, and B. Farago, Europhys. Lett. **7**, 529 (1988).

[46] J. N. Roux, J. L. Barrat, and J. P. Hansen, J. Phys. Condens. Matter **1**, 7171 (1989).

[47] G. F. Signorini, J. L. Barrat, and M. L. Klein, J. Chem. Phys. **92**, 1294 (1990).

[48] G. Li, W. M. Du, X. K. Chen, and H. Z. Cummins, Phys. Rev. A **45**, 3867 (1992).